

Hardware realization of collision avoidance method in VLF-LF frequency bands in mine conditions

*Timur V. Krasnov**, *Viacheslav V. Romanov*, and *Ekaterina A. Kohonkova*

Siberian Federal University, Krasnoyarsk, Russia

Abstract. The paper proposes a method of measuring the distance between mining equipment and workers in complex conditions of underground mine workings considering the influence of absorbing properties of rocks and the presence of turns and obstacles. The method consists in using a magnetic beacon, operating in VLF-LF frequency range, on the body of mining equipment and receivers on the miner's body to register proximity and notify a person about it. Registration of convergence is carried out by RSSI methods. The authors propose a design solution of magnetic beacon and receiver, which includes amplification stages for signal registration at 30-35 meters. The paper also presents the measurement error of the information parameter under the influence of the ground surface and the tunnel.

1 Introduction

The development of underground and surface mining methods requires the use of a large amount of equipment for the extraction and transportation of minerals, tools and workers (transport vehicles, bulldozers, dump trucks, front-end loaders, load-and-haul dump trucks, dump trucks and excavators). In many mining countries, fatal accidents involving transport and mobile equipment occur in 16-48%, depending on the region [1]. Numerous studies [2-4] show that mining equipment and vehicles are the main source of injuries in the mining industry after rock falls.

There are many devices available in the mining industry that can identify people and vehicles in the vicinity of a mining machine, but they have their own specific limitations. Positioning in land-based mining operations uses the method of joint operation of a global satellite navigation system and a stationary positioning station located on a tower and connected to the enterprise's local network. When changing the location of mining equipment and personnel to underground mine workings, it is necessary to use other approaches to prevent collisions and run-overs [5-8].

To solve this problem, it is possible to use several different distance measurement principles [9–13]. ToA, TDoA and AoA distance determination methods require synchronization of base stations in time and/or their stationary location in space, which increases the cost of providing the mine with full coverage of such a positioning system, and

* Corresponding author: krasnovtv@ya.ru

also does not allow for a quick response due to the large number of processing and receiving nodes decisions.

The ToF method is the most portable and does not require stationary time-synchronized base stations. The distance is calculated using the time of flight of the pulse between two radio modules, since the speed of an electromagnetic wave in air is a constant value. The method operates in the UHF and microwave range, which also makes the system vulnerable to environmental influences. In the conditions of rocks with an electrical conductivity of $0.001 \div 0.1$ S/m, the absorption and reflection of high-frequency EM waves from walls and their scattering remain relevant. If the person with the radio module is positioned outside the line of sight, such as an obstacle or turning into an adjacent tunnel, it may lead to loss of signal or incorrect data exchange between the mining equipment module and the miner module.

As an alternative or additional support for the proximity detection system at close range (closer than 30 m), it is proposed to use low-frequency magnetic fields (VLF, LF range), which are more resistant to the influence of rocks composing the walls and roof of tunnels. Operation in this frequency range involves the use of the RSSI algorithm.

2 Materials and methods

To prevent collisions between equipment and personnel, the authors propose to use the RSSI method, which is most suitable for the VLF and LF range due to the operation of the system in the near zone of the emitter. It is based on the use of a device in the form of a magnetic beacon with an antenna based on a multi-turn coil, installed on the front and rear of mining machines. The distribution diagram of the magnetic field in space for such an antenna is close to an isotropic magnetic emitter and has no local minima. The field of a magnetic antenna oriented along the X axis includes axial (H_x) and radial (H_y , H_z) components distributed in space as shown in Figure 1 a-c. To register all components of the transmitter's magnetic field, forming the total field H (Figure 1d), it is necessary to integrate a complex antenna into the receiving path, which includes three magnetic antennas oriented orthogonally to each other.

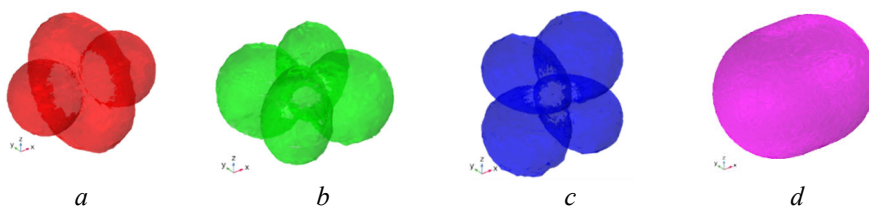


Fig. 1. Distribution of the magnetic field components of the beacon antenna in three-dimensional space: a – axial H_x ; b – radial H_y ; c – radial H_z ; d – normalized H .

A method for preventing collisions between equipment and workers involves placing a magnetic beacon on the body of the vehicle and an individual receiver on the miner's body, which registers the degree of his proximity to the equipment according to the principle of zoning, determined by distance (Figure 2):

- Distance >30 m – “green zone” area of attention;
- Distance 30-15 m – “yellow zone”, the area of dangerous proximity;
- Distance <15 m – “red zone”, the area of probable accident.

When crossing the boundary of the attention zone, the receiving device must signal the worker about the approach of the equipment through vibration, light or sound signal. The mine workings have a cross-section with an area of 4 to 25 m² in square, rectangular and arched shapes. Also in mines, wide galleries for the production of ore and minerals are

common with the presence of pillars to support the arch of rock with dimensions of 1.5-4 m and an average interval of 5 m, which limits the line of sight for miners and equipment operators, as well as high-frequency recording methods bringing technology and workers closer to each other.

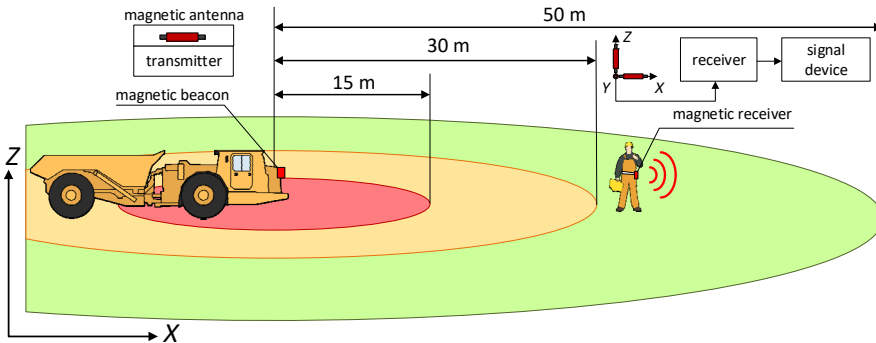


Fig. 2. Diagram of implementation of the collision avoidance method.

When operating in the VLF and LF range in mining conditions, the magnetic field of the emitter undergoes the least absorption of energy by the rocks of the walls and roof of the mine and the subsequent distortion of the magnetic field strength diagram, which leads to an error in determining the distance using the RSSI method. This error, which is unpredictable, is introduced into the system under the influence of the electrical conductivity of the tunnel rocks because of magnetic field absorption. This parameter varies within $5 \cdot 10^{-5} \div 10^{-1}$ S/m and depends on the geology and hydrogeology of the mine. Analysis of the degree of this influence is realized through computational modeling [14]. The propagation of the magnetic field of a beacon attached to the front part of the body of a truck model in a mining opening was modeled with a change in electrical conductivity from 10^{-3} to 0.1 S/m (the parameter changes when moving from openings in the host rocks to ore layers) for frequencies 8, 35, 125 kHz. When a magnetic beacon operates in a mine working with a scatter of electrical conductivity values, the error in measuring the distance by signal level reaches 1 m at a frequency of 8 kHz at 27-30 m, which is the most optimal option. As the operating frequency of the beacon increases, the error also increases due to the frequency dependence of the absorption of the magnetic field by the rock. Thus, at a frequency of 35 kHz, the maximum change in the electrical conductivity of rocks gives a distance measurement error of 1 m at 12-13 m.

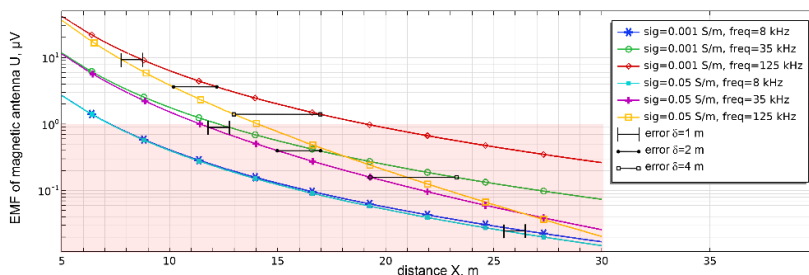


Fig. 3. Dependence of the signal level at the receiving antenna U on distance for frequencies 8 kHz, 35 kHz, 125 kHz and electrical conductivity 0.001 S/m and 0.05 S/m in a mine working.

The proposed system uses a method for determining the RSSI distance using amplitude modulation of the signal. To do this, the device includes two local oscillator modules that

generate oscillations at the carrier and modulating frequencies, which are fed to the mixer to obtain a modulated signal (Figure 4a). The modulated signal has a modulation depth of $M=80\%$ and is fed to an amplifier (TDA7294) with a gain $K_{us}=30$, which is powered by a portable battery with $U_p=12\text{ V}$ through a power source. The output signal is fed to a transformer made based on a PQ35/35 core, which matches the output stage of the amplifier with the oscillating circuit of the radiating antenna (Figure 4a), tuned to the resonant frequency corresponding to the carrier $f_0=8\text{ kHz}$ ($L_A=3.95\text{ mH}$, $C_A=100\text{ nF}$).

The transmitting antenna includes a coil of 10 turns based on a core with a rectangular cross-section of $20\times 25\text{ mm}$ and a length of 200 m , the core material is ferrite with $\mu=700$ (Figure 4b).

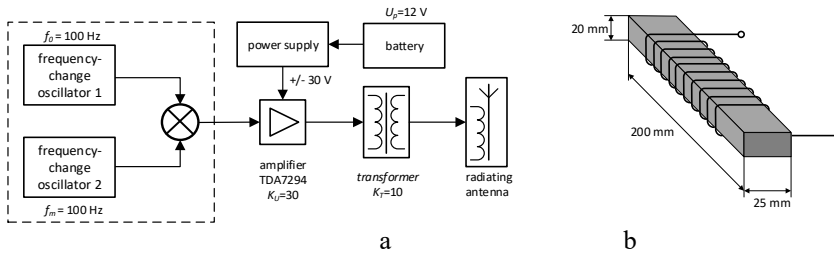


Fig. 4. Block diagram of a low-frequency magnetic transmitter (a) and appearance of a radiating magnetic antenna (b).

The use of amplitude modulation solves two main problems:

- 1) Increasing the noise immunity of the communication channel by highlighting the low-frequency envelope and separating the high-frequency component of the carrier signal in the receiving path.
- 2) Identification of a tag installed on a vehicle body by its envelope frequency.

The determination of the distance is also calculated through the amplitude of the envelope, which decreases in proportion to the amplitude of the carrier signal at the output of the receiving magnetic antenna with distance from the radiating antenna of the magnetic beacon according to a cubic dependence:

$$L = \sqrt[3]{\frac{e_{L0}}{e_m}} \cdot L_0 \quad (1)$$

where e_{L0} - EMF at the receiver input at the calibration point at a distance from the radiating antenna, at which the amplifiers in the receiver reach the limiting mode;

e_m - EMF measured at the output of the receiving antenna,

$$e_m = \frac{U_{amp_out}}{Q \cdot K_U \cdot h_{eff} \cdot 10^3} \quad (2)$$

where U_{amp_out} - output voltage of amplification stages; Q - antenna quality factor; h_{eff} - effective receiving antenna height; K_U - amplifier end-to-end gain; $K_T=10$ antenna transformation ratio.

Due to the extremely strong drop in the magnetic field strength of a multi-turn coil with distance from the emitter, it is necessary to solve the design problem of increasing the sensitivity of the receiver to increase the coverage area to a radius of more than 30 m . This is realized by including controlled amplification stages in the circuit. The receiver mounted on the miner's body (Figure 5) includes a magnetic ferrite antenna tuned to the resonance of the carrier frequency $f_0=8\text{ kHz}$, with a quality factor of the oscillating circuit $Q=70$. The antenna is connected to the amplifier through a cascade that ensures matching of the receiving antenna circuit with the input impedance of the amplifier. Also, the matching stage ensures direct current operation for subsequent amplifier stages, which minimizes the manifestations

of transient processes, because they are consistent with each other. The mode of full inclusion of the antenna oscillating circuit eliminates the influence of the amplification matching stage on the quality factor Q of the antenna, the large value of which ensures the narrowbandness of the receiving path. This eliminates the need to introduce frequency-dependent elements into the feedback circuit of the amplifier stages.

To increase the registration distance of a magnetic beacon signal, it is necessary to increase the sensitivity of the receiving device. For this purpose, the amplification path includes two stages built on operational amplifiers, organized according to a non-inverse classical switching circuit with a variable gain. The amplified input signal is sent to the ADC of the MCU microcontroller, where analog-to-digital conversion, detection and extraction of the envelope occurs, followed by distance calculation. The gain of the cascades is adjusted by the microcontroller using digital potentiometers based on their values of the maximum and minimum signal levels at the amplifier output. A number written into the potentiometer register of each gain stage, which corresponds to a certain value of resistance of the digital potentiometer, and, accordingly, the value of the gain. Based on the calculated distance, the MCU evaluates the degree of proximity to the magnetic beacon and activates the signaling device in accordance with the algorithm.

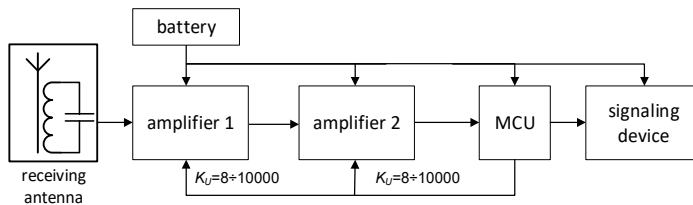


Fig. 5. Block diagram of the receiver and matching circuit of the antenna with the amplification stage.

The use of two amplification stages makes it possible to obtain an amplifier with a large dynamic range $K_L=8+10000$ ($k=0+255$), which is necessary for processing and digitizing the signal under conditions of an intensive decrease in the level of magnetic field strength with distance according to the law $H \sim 1/L^3$. Near the emitting antenna, the signal does not require amplification, but as the distance between the transmitter and receiver increases, the signal level drops below the threshold value and the need for amplification arises for conversion and detection.

The resonant frequency of the receiving circuit is determined from the equation:

$$f_0 = \frac{1}{2\pi\sqrt{L_{WA1}C_P}} \sqrt{\frac{\rho^2 - R_{LWA1}}{\rho^2 - R_{CP}}} \tag{3}$$

where ρ – characteristic impedance;

R_{LWA1} – antenna resistance;

R_{CP} – active resistance of the matching capacitance;

L_{WA1} – antenna inductance;

C_P – antenna matching capacitance value.

Antenna characteristic impedance:

$$\rho = \sqrt{\frac{L_{WA1}}{C_P}} \tag{4}$$

Antenna circuit quality factor:

$$Q = \sqrt{\frac{\rho}{R}} \tag{5}$$

where $R=R_L+R_C$ –amount of active losses.

Since the equivalent active resistance, which serves as a load for the receiving antenna circuit, exceeds 10 MOhm, its influence on the circuit is not significant and can be neglected.

Considering the installed elements, the receiving antenna circuit has a characteristic impedance:

$$Z = \frac{\rho^2}{R} = \frac{LWA_1}{C_{PR}}, \tag{6}$$

Where the excitation current of the circuit can be determined according to the relationship:

$$I_{ex} = \frac{e_a}{Z}, \tag{7}$$

where e_a – EMF induced at the receiving antenna (coil).

Therefore, the operating (resonant) current of the circuit is determined as:

$$I_r = I_{ex} \cdot Q, \tag{8}$$

This way the voltage value of the circuit that is in resonance can be determined:

$$U_{con} = I_r \cdot Z, \tag{9}$$

The cascade that performs the function of matching the antenna with the amplification path has a fixed gain:

$$K_U = 1 + \frac{R_{13}}{R_{12} + X_{C_{11}}} = 1.98, \tag{10}$$

where $X_{C_{11}} = 1/(2 \cdot \pi \cdot f_0 \cdot C_{11}) = 200$ Ohm.

Resistance R10 and R11 form a divider with a division factor of 2 and form an artificial midpoint, i.e. DC bias of the cascade through the antenna coil winding. This voltage is repeated at the output of the amplifier and serves as a reference voltage for subsequent stages, because each amplifier stage has a DC gain equal to 1. The gain is taken into account when calculating the distance and is determined based on the ratios:

$$K_U = 1 + \frac{R_3}{R_{DA1} + X_{C_2}}, \tag{11}$$

where $X_{C_2} = 1/(2 \cdot \pi \cdot f_0 \cdot C_2)$

$R_{DA1} = 890 \div 51300$ Ohm – the resistance of a digital potentiometer is determined by the number stored in the memory of its register;

$C_2 = 100$ nF.

Since the amplifier stages have the same structure, this relationship is also valid for the second stage. The end-to-end gain is defined as the product of the gains of each of the three stages.

Processing of the amplified signal and extraction of the envelope is provided based on the MCU controller (Figure 6).

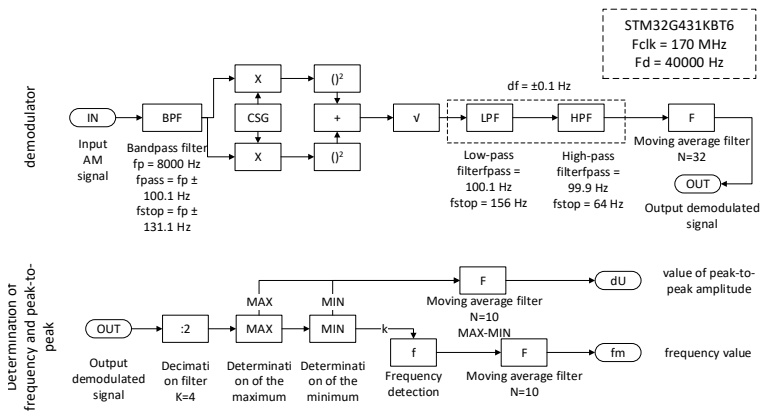


Fig. 6. Block diagram of a digital receiver based on MCU.

The digital detector is built on the quadrature detection method. The input signal is fed to a bandpass filter with a center frequency of 8 kHz to isolate the band with the desired signal and suppress low-frequency components. Next, the quadrature components of the signal are formed using a tabular cosine-sine generator (KSG), where tables of values of 1 period of cosine and sine are generated with a sampling frequency of 40 kHz. To isolate the envelope, the quadrature components are squared, summed, and the square root is taken from the sum. The envelope signal is fed to a low pass filter (LPF) and a high pass filter (HPF). The moving average filter filters out random noise. The output signal is fed to a block for selecting frequency and signal range.

Since the amplifier stages have the same structure, this relationship is also valid for the second stage. The end-to-end gain is defined as the product of the gains of each of the three stages.

3 Results and discussion

When moving to more than 5 m, the error in determining the distance is set at the same level and increases linearly with distance. This allows you to introduce correction factors into the distance determination algorithm to determine the distance with a minimum error. The medium introduces an error into the distance determination by the RSSI method, but at a frequency of 8 kHz this influence is minimized. Depending on the circumstances, such as changing the location of the vehicle from the surface to the mine workings, it is necessary to consider correction factors depending on the influence of the environment on the propagation of the magnetic field. These coefficients are selected based on modeling and static data obtained during experiments.

Considering the specific nature of magnetic field radiation, the transmitting device has a high energy consumption. From this it follows that a magnetic beacon can be installed on the body of mining or transport equipment. The complete set of the transmitter is shown in Figure 7 a. The transmitter and internal magnetic antenna based on a ferrite core are mounted in the housing, external antennas for alternative configurations are connected via terminals. It is proposed to place the receiving device on the worker's equipment and connect it to a signaling device to warn of proximity to equipment by means of a sound signal and/or vibration. The modification shown in Figure 1 is used as a receiving device for recording experimental data. 7 b, with the function of adjusting the gain and analyzing the carrier and modulating frequencies of the received signal.

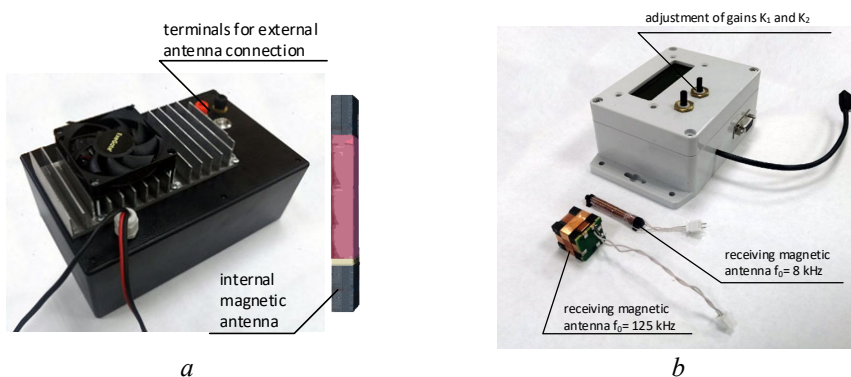


Fig. 7. Signal transmission and reception devices: a – prototype of a transmitter and a transmitting magnetic antenna on a ferrite core; b – prototype receiver and receiving ferrite antennas.

The receiving device and antenna are installed in the housing; gain adjustment is done manually. The digital display displays information about the frequency of the received signal and the value of the gain factors, as well as the voltage at the output of the receiver's ADC. Receiving antennas are made for a frequency of 8 kHz (single-component antenna, number of turns $n=4000$) and 125 kHz (three-component antenna in the form of three orthogonal coils, number of turns $n=43$).

4 Conclusion

Analysis of the propagation of the magnetic field of the VLF-LF range under the influence of conductive media showed that the use of this frequency range in conjunction with the RSSI algorithm is the most stable method for determining distance in underground mine workings. Reducing the operating frequency to 8 kHz makes it possible to reduce the influence of rocks with electrical conductivity in the range of $10-3 \div 0.05$ S/m on the error in determining the distance to 1 m at 27 m from the emitter. Also, the low-frequency magnetic field is stable against the influence of rocks and allows you to detect the approach of mobile equipment outside the line of sight. To register the beacon's magnetic field, it is necessary to use three orthogonal receiving magnetic antennas. In general, this method can be used as a warning system about dangerous proximity of mining equipment to each other and for miners and due to the high energy consumption of the signal beacon. Once within the beacon's influence zone, the receiving device signals the intersection of certain areas at a fixed distance by means of a sound signal and/or vibration.

The reported study was funded by Krasnoyarsk Regional Fund of Science and LLC «Radiotechnic systems» according to the research project «Development of a collision and personnel hitting prevention system for large-sized mining-transport equipment based on the combined use of ultra-wideband signals and low-frequency electromagnetic waves».

References

1. M. Imam, K. Bařna, Y. Tabii et al. *Sensors* **23(9)** 4294 (2023)
2. P. Strzalkowski, *IOP Conference Series: Earth and Environmental Science* **362** 012033 (2019)
3. E. Rahimia, Y. Shekariana, N. Shekarian, P. Roghanchi, *Journal of Sustainable Mining* **21(1)**, 27-44 (2022)
4. V.S. Oksman, N.K. Trubetskoy, A.I. Grazhdankin, *Labor safety in industry* **3** 28-35 (2021)
5. J. Shahmoradi, E. Talebi, P. Roghanchi, M. A Hassanalian, *Drones* **4**, 34 (2020)
6. M. Patrucco, E. Pira, S. Pentimalli, R. Nebbia, A. Sorlini, *Infrastructures* **6**, 42 (2021)
7. J. Dickens, J. Green, et al., *Global Survey of Systems and Technologies Suitable for Vehicle to Person Collision Avoidance in Underground Rail-Bound Operations* (Mine Health and Safety Council: Woodmead, South Africa, 2014)
8. M. Patrucco, E. Pira, S. Pentimalli, R. Nebbia, A. Sorlini, *Infrastructures* **6**, 42 (2021)
9. Z. Zhou, J. Zhang, C. Gong, *Comput.-Aided Civ. Infrastruct. Eng.* **37**, 762-780 (2022)
10. H. Kai, M. Xianmin, Research on avoidance obstacle strategy of coal underground inspection robot based on binocular vision. In *Proceedings of the 2017 29th Chinese Control And Decision Conference (CCDC)*, China, 2017, pp. 6732-6737

11. S. Adam, B. Coward, G. DeBerry, C. Glazier, E. Magnusson, M. Boukhechba, Investigating Novel Proximity Monitoring Techniques Using Ubiquitous Sensor Technology. In Proceedings of the 2021 Systems and Information Engineering Design Symposium (SIEDS), USA, 2021, pp. 1-6
12. Z. Wang, G. Xu, M. Zhang, Y. Guo, Collision Avoidance Models and Algorithms in the Era of Internet of Vehicles. In Proceedings of the 2020 IEEE 3rd International Conference of Safe Production and Informatization (IICSPI), China, 2020, pp. 123–126
13. R. Ali, R. Liu, Y. He, A. Nayyar, B. Qureshi, IEEE Access **9**, 122924-122950 (2021)
14. N. B. Dortman, *Physical Properties of the Rocks and Mineral Resources* (Nedra, Moscow, 1984)